Int. J. Heat Mass Transfer. Vol. 34, No. 10, pp. 2663–2668, 1991
Printed in Great Britain

0017-9310/91 $3.00 + 0.00

TECHNICAL NOTES

Temperature visualizations by use of liquid crystals of unsteady natural convection during supercooling and freezing of water in an enclosure with lateral cooling

TATSUO NISHIMURA
Department of Mechanical Engineering, Yamaguchi University, Ube 755, Japan

and

MASAKI FUJIWARA, NAMIKO HORIE and HISASHI MIYASHITA
Department of Materials Science and Engineering, Toyama University, Toyama 930, Japan

(*Received* 19 *October* 1990)

1. INTRODUCTION

IN RECENT years, optical methods such as Mach–Zehnder and holographic interferometers have been used to study the pattern of unsteady natural convection in the processes of supercooling and freezing of water. Tankin and Farhadieh [1] first used a Mach–Zehnder interferometer to study the formation of ice from above or from below. Kashiwagi *et al.* [2] studied flow and heat transfer characteristics of water with a supercooled region using a holographic interferometer. Fukusako and Takahashi [3] investigated the influence of density inversion of water in the natural convection heat transfer of air–water layers within a cooled circular tube. A holographic interferometry technique was adopted to determine the time-dependent temperature field in the tube. Narumi *et al.* [4] used the same technique to study the supercooling of water in double horizontal concentric cylinders.

Although the optical methods give information on spatial variations of isotherms, accurate measurements of temperature distributions near 4°C are difficult, because the variations in density and refractive index of water with temperature are very small in this region. Numerical studies of water supercooling or freezing without supercooling predict that the isotherms near 4°C play an important role in unsteady natural convection with density inversion [5–7]. However, this has not been confirmed experimentally because of the difficulties of measuring these temperatures by optical methods. Previous studies have also not shown how, for lateral cooling, the pattern of natural convection changes with the release of supercooling, although recently Brewster and Gebhart [8] studied natural convection effects on supercooling and subsequent freezing for downward cooling by a flow visualization technique. These problems motivated the present investigation.

Here we attempted to observe the isotherms near 4°C during freezing of water by encapsulated thermochromic liquid crystals. Recently, temperature fields for thermal convection have been visualized by use of cholesteric liquid crystals suspended in fluids [9, 10]. However, because it is difficult to visualize temperatures for water using cholesteric liquid crystals, we adopted another liquid crystal, i.e. a chiral nematic type, which we had previously confirmed to be useful for temperature visualizations for water [11].

This work uses the liquid crystal to examine the fundamental heat transfer processes that accompany supercooling and subsequent freezing of water contained in an enclosure with lateral cooling.

2. EXPERIMENTAL APPARATUS AND PROCEDURE

Figure 1 shows a schematic diagram of the experimental apparatus. Experiments were performed in a rectangular test cell with the following inner dimensions: 40 mm long, 50 mm high and 30 mm wide. The test cell was made of acrylic resin, except for the cold wall, which consisted of a copper plate. A cooling chamber was attached to the rear side of the cold wall, and the wall temperature was maintained below 0°C by refrigeration unit 1. Refrigeration unit 2 was used to control the initial temperature of water. To minimize heat losses, the test cell was insulated with 60 mm of styrofoam on all sides, and the experimental apparatus was placed in a temperature-controlled room. Four copper–constantan thermocouples of 100 μm in diameter were located at the mid-height of the test cell as shown in Fig. 1.

Liquid crystals change color according to the environmental temperature, and this change is reversible and repeatable as long as the liquid crystals are not physically damaged. The liquid crystals used here were manufactured by BDH Chemicals Ltd., Poole, England, and were chosen to cover a temperature range from 2.5 to 5°C in order to focus on the density inversion process of water. The corresponding colors ranged from red at the bottom of the temperature range, through yellow and green, to blue at the top. The density of encapsulated liquid crystals was about 1.02×10^3 kg m^{-3} and their diameter ranged from 10 to 15 μm. The amount of liquid crystals suspended in pure water (0.002 vol%) was one-tenth of the amount of cholesteric liquid crystals needed. The time constant for the temperature variation of the liquid crystals is about 0.3 s, and therefore the delay of their response to temperature change is probably small for the flow field of laminar natural convection considered here. Light was introduced through a slit by a 300 W projector lamp. Time-dependent temperature fields were photographed with an exposure time of 0.5 s.

Flow patterns were also observed by use of a dye tracer, the encapsulated liquid crystals used being unsuitable for this purpose because of their small diameter and the decay of natural convection with the progression of freezing.

NOMENCLATURE

c_l	specific heat for water
c_s	specific heat for ice
Fo	Fourier number, $\alpha_s t/L^2$
H	height of the enclosure
ΔH	latent heat
L	length of the enclosure
s	superheating parameter, $c_l(T_i - T_f)/\Delta H$
Ste	Stefan number, $c_s(T_f - T_c)/\Delta H$
T	temperature
T_c	temperature at the cold wall
T_f	freezing temperature, 0°C
T_i	initial water temperature
T_j	peak temperature
T_n	nucleation temperature
t	time
V	ice volume
V_0	volume of the enclosure
W	width of the enclosure.

Greek symbols

α_s	thermal diffusivity for ice
ρ	density.

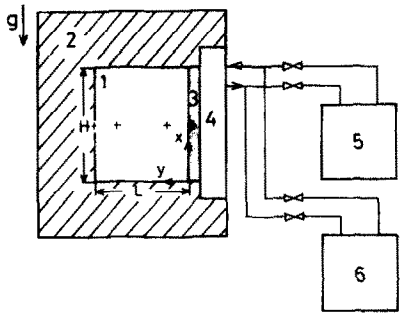

FIG. 1. Experimental apparatus: 1, test section; 2, styrofoam insulation; 3, copper plate; 4, cooling chamber; 5, refrigeration unit 1; 6, refrigeration unit 2. $H = 50$ mm, $L = 40$ mm. +, position of thermocouples.

3. EXPERIMENTAL RESULTS AND DISCUSSION

Figure 2 shows temperature variations with time at several positions in the test cell as measured by use of the thermocouples, for $T_i = 25$°C and $T_c = -14.6$°C. The symbols (○, ○, □, △) in the schematic diagram of the test cell, also shown in Fig. 2, indicate the positions of the respective thermocouples. Photographs of the corresponding time-dependent temperature fields revealed by the liquid crystals and schematic flow patterns shown by the dye tracer are shown in Figs. 3 and 4, respectively. The green color of the liquid crystal corresponds approximately to the maximum density temperature of water.

Comparison of Figs. 2–4 affords an insight into the flow and temperature fields in the processes of water supercooling and subsequent freezing. Initially, the cold wall temperature fell abruptly as shown in Fig. 2, since the heat exchanger was suddenly exposed to the cold circulation fluid. When the temperature fell below 0°C, water in the vicinity of the cold wall was supercooled until nucleation occurred. At the instant of nucleation, 6 min 9 s after the start of the experiment, the temperature jumped from the nucleation temperature $T_n = -9.0$°C to a peak value of $T_j = -6.9$°C. The time-dependent temperature and flow fields during supercooling are shown in Parts (a)–(e) of Figs. 3 and 4, respectively.

At the beginning of supercooling, there was a marked lowering of temperature at all positions as shown in Fig. 2. This resulted from natural convection by the clockwise vortex depicted in Fig. 4. Even at this stage, isotherms near 4°C indicate that, in addition to the clockwise vortex, a small counter-clockwise vortex had appeared near the lower portion of the cold wall, marking the beginning of the density inversion process (see Figs. 3(a) and 4(a)).

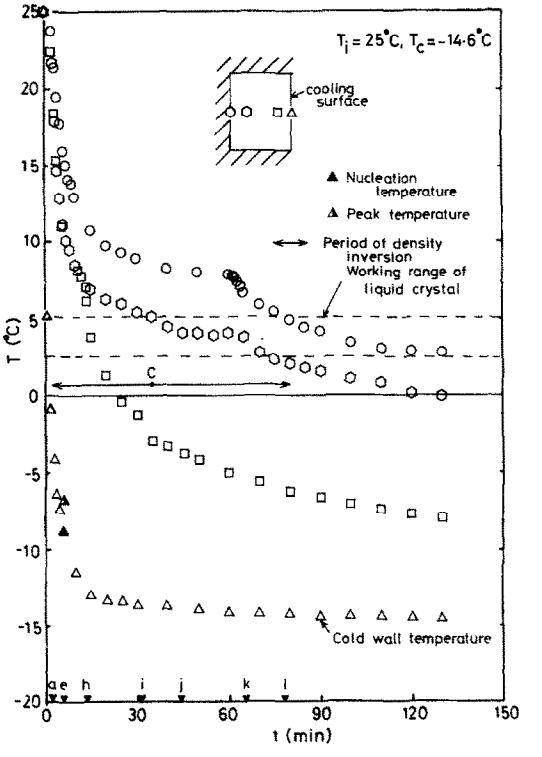

FIG. 2. Temperature histories during freezing for $T_i = 25$°C and $T_j = -14.6$°C.

With the progression of supercooling, the counter-clockwise vortex gradually grew along the cold wall (see Parts (b)–(d) of Figs. 3 and 4). The interface between the two counter-rotating vortices corresponds approximately to the isotherm near 4°C.

In Figs. 3(e) and 4(e) dendritic ice has been formed at the top of the counter-clockwise vortex, where the water was coldest. The dendritic ice consisted of thin, plate-like crystals interspersed in the water medium, and it grew obliquely against the cold wall due to the counter-clockwise vortex. Subsequently, the counter-clockwise vortex rapidly disappeared because of the dramatic decrease in the buoyancy force of water by the release of supercooling, and simultaneously the dendritic ice disappeared, leaving a pure ice layer on the cold wall (see Parts (f) and (g) of Figs. 3 and 4).

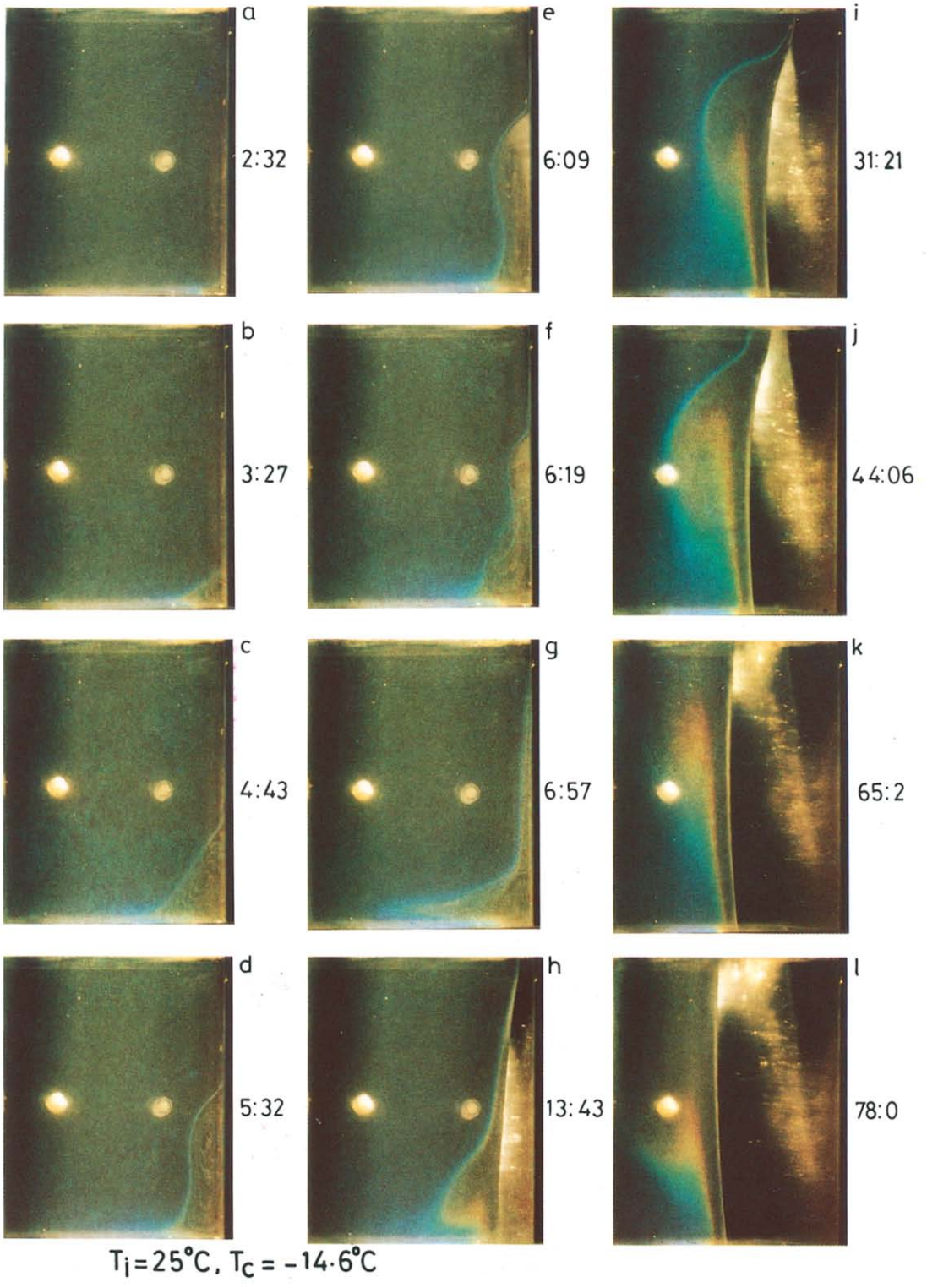

FIG. 3. Temperature visualization photographs.

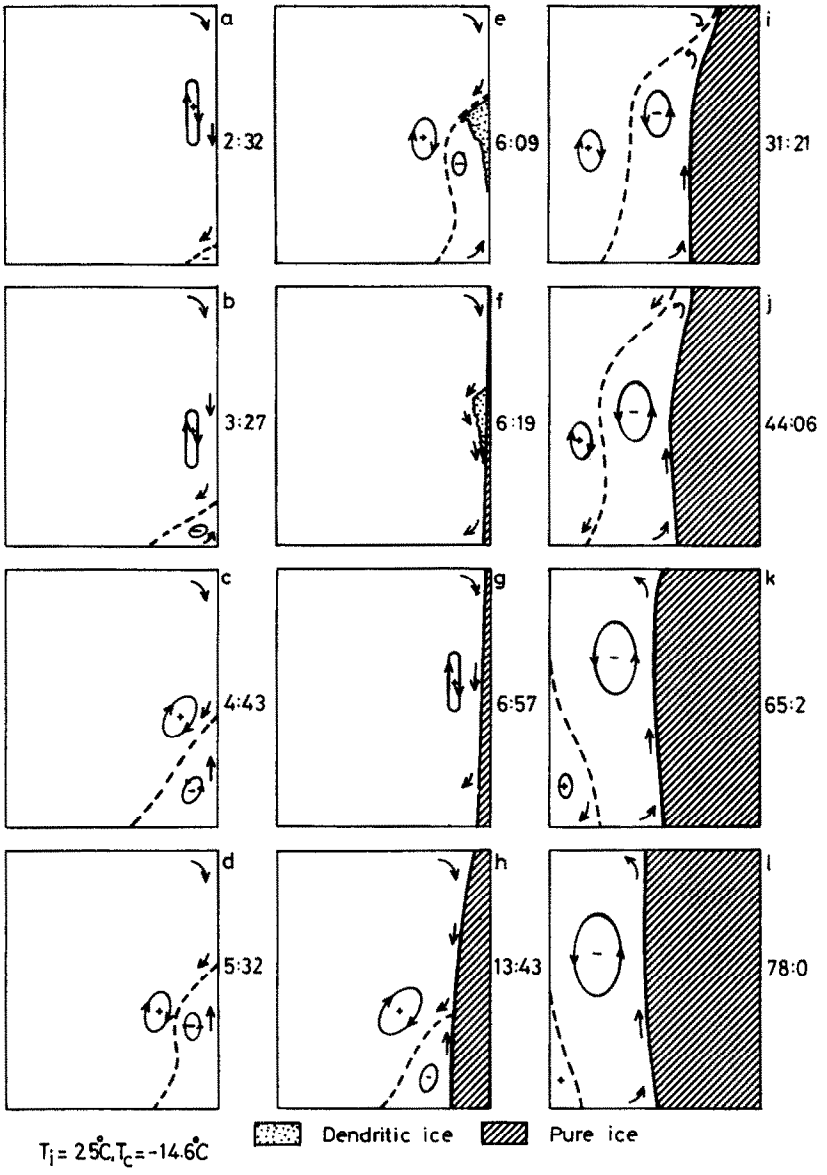

FIG. 4. Schematic flow patterns.

With the progression of freezing, the clockwise vortex reappeared at the bottom of the water/ice interface, then extended upwards to cover the interface (see Parts (h)–(j) of Figs. 3 and 4). Point C in Fig. 2 represents the time at which the entire water/ice interface became covered by the counter-clockwise vortex. At this time, we suggest that the strength of the counter-clockwise vortex is almost identical to that of the clockwise vortex. Within the clockwise vortex separated from the water/ice interface, temperature changed slowly with time due to the combined action of the two counter-rotating vortices, as shown by the points marked ○ and ○ in Fig. 2.

As freezing progressed further, the counter-clockwise vortex exceeded the clockwise vortex and the temperatures marked ○ and ○ in Fig. 2 decreased again. At time $t = 78$ min, the clockwise vortex was almost completely engulfed by the counter-clockwise vortex, as shown in Figs. 3(l) and 4(l), indicating that the density inversion process had come to an end. Thereafter, the results in Fig. 2 show that, as expected, the fluid motion by the counter-clockwise vortex becomes increasingly minute due to a decrease of liquid superheat.

In the foregoing section, we have visualized the complex heat transfer processes that accompany the release of supercooling. These have not been clearly observed by such optical methods as the use of Mach–Zehnder and holographic interferometers, and thus the chiral nematic liquid crystals used here were found to be useful for temperature visualizations in the density inversion process of water. The temperature visualizations will be used to allow for quantitative comparison with the numerical calculations which are currently established.

In terms of ice growth, the effect of natural convection by the clockwise vortex is manifested at the beginning of freezing by the retardation of ice growth at the top of the test cell. However, with the progression of freezing, ice growth is

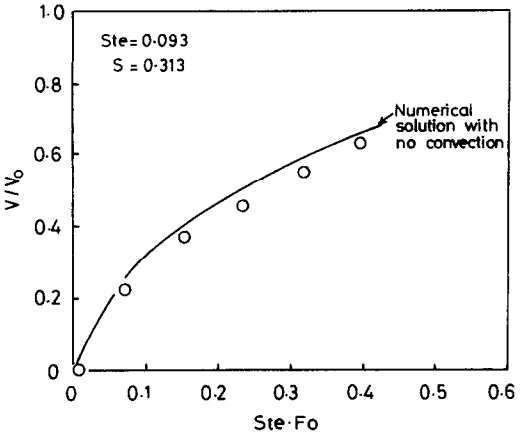

FIG. 5. Variation of ice volume with time.

suppressed at the base of the test cell due to density inversion. The non-uniform ice growth in the horizontal direction is clearly shown in Figs. 3(h)–(l). The total volume of ice formed was determined by integrating the contours of the water/ice interface shown in the photographs of Fig. 3. Figure 5 shows the result. The solid line also shown in this figure is a numerical solution without supercooling and natural convection. The numerical solution was obtained by the finite element method used in the previous study [12]. There is evidence that natural convection plays an important role in determining the ice volume in the presence of large liquid-phase initial superheat, as expected from the shape of the water/ice interface described above.

REFERENCES

1. R. S. Tankin and R. Farhadieh, Effects of thermal convection currents on formation of ice, *Int. J. Heat Mass Transfer* **14,** 953–961 (1971).
2. T. Kashiwagi, S. Hirose, S. Itoh and Y. Kurosaki, Effects of natural convection in a partially supercooled water cell on the release of supercooling, *Trans. JSME Ser. B* **53,** 1822–1827 (1987).
3. S. Fukusako and M. Takahashi, Free convection heat transfer of air–water layers in a cooled circular tube, *Bull. Fac. Engng Hokkaido Univ.* **146,** 21–32 (1989).
4. A. Narumi, T. Kashiwagi and Y. Sakatoku, Cooling and freezing process of water with a supercooled region in the double horizontal concentric cylinders, *Trans. JSME Ser. B* **56,** 2077–2084 (1990).
5. K. C. Cheng, M. Takeuchi and R. R. Gilpin, Transient natural convection in horizontal water pipes with maximum density effect and supercooling, *Numer. Heat Transfer* **1,** 101–115 (1978).
6. L. Robillard and P. Vasseur, Transient natural convection heat transfer of water with maximum density effect and supercooling, *Trans. ASME J. Heat Transfer* **103,** 528–534 (1981).
7. M. Hattori, Heat transfer with freezing and/or melting, *Refrigeration* **62,** 362–368 (1987).
8. R. A. Brewster and B. Gebhart, An experimental study of natural convection effects on downward freezing of pure water, *Int. J. Heat Mass Transfer* **31,** 331–348 (1988).
9. T. Munakata and I. Tanasawa, A study of the onset of oscillatory flow in a Czochralski growth and its suppression by a magnetic field, *Trans. JSME Ser. B* **55,** 2610–2617 (1989).
10. Y. Shiina, N. Akino, T. Kunugi and K. Fujimura, Visualization of flow and temperature fields of natural convection in a hemisphere heated from below, *J. Visualization Soc. Japan* **10,** 41–46 (1990).
11. T. Nishimura, M. Fujiwara and H. Miyashita, Visualization of temperature fields of transient natural convection with maximum density effect in a water-filled enclosure by chiral nematic liquid crystals, *J. Chem. Engng Japan* **23,** 241–244 (1990).
12. T. Nishimura, S. Itoh, H. Tsuboi and Y. Kawamura, Analysis of two-dimensional freezing by the finite element method, *Int. Chem. Engng* **25,** 105–112 (1985).